RESEARCH ARTICLE

Analysis of Two-Component Systems in Group B *Streptococcus* Shows That RgfAC and the Novel FspSR Modulate Virulence and Bacterial Fitness

Cristina Faralla,[a] Matteo M. Metruccio,[a]* Matteo De Chiara,[a] Rong Mu,[b] Kathryn A. Patras,[b] Alessandro Muzzi,[a] Guido Grandi,[a] Immaculada Margarit,[a] Kelly S. Doran,[b] Robert Janulczyk[a]

Novartis Vaccines, Siena, Italy[a]; Department of Biology and Center for Microbial Sciences, San Diego State University, San Diego, California, USA[b]

* Present address: Matteo M. Metruccio, School of Optometry, University of California, Berkeley, Berkeley, California, USA.

M.D.C., R.M., and K.A.P. contributed equally to the work and are listed in alphabetical order.

ABSTRACT **Group B *Streptococcus* (GBS), in the transition from commensal organisms to pathogens, will encounter diverse host environments and, thus, require coordinated control of the transcriptional responses to these changes. This work was aimed at better understanding the role of two-component signal transduction systems (TCS) in GBS pathophysiology through a systematic screening procedure. We first performed a complete inventory and sensory mechanism classification of all putative GBS TCS by genomic analysis. Five TCS were further investigated by the generation of knockout strains, and *in vitro* transcriptome analysis identified genes regulated by these systems, ranging from 0.1% to 3% of the genome. Interestingly, two sugar phosphotransferase systems appeared to be differentially regulated in the TCS-16 knockout strain (TCS loci were numbered in order of their appearance on the chromosome), suggesting an involvement in monitoring carbon source availability. High-throughput analysis of bacterial growth on different carbon sources showed that TCS-16 was necessary for the growth of GBS on fructose-6-phosphate. Additional transcriptional analysis provided further evidence for a stimulus-response circuit where extracellular fructose-6-phosphate leads to autoinduction of TCS-16, with concomitant dramatic upregulation of the adjacent operon, which encodes a phosphotransferase system. The TCS-16-deficient strain exhibited decreased persistence in a model of vaginal colonization. All mutant strains were also characterized in a murine model of systemic infection, and inactivation of TCS-17 (also known as RgfAC) resulted in hypervirulence. Our data suggest a role for the previously unknown TCS-16, here named FspSR, in bacterial fitness and carbon metabolism during host colonization, and the data also provide experimental evidence for TCS-17/RgfAC involvement in virulence.**

IMPORTANCE **Two-component systems have been evolved by bacteria to detect environmental changes, and they play key roles in pathogenicity. A comprehensive analysis of TCS in GBS has not been performed previously. In this work, we classify 21 TCS and present evidence for the involvement of two specific TCS in GBS virulence and colonization *in vivo*. Although pinpointing specific TCS stimuli is notoriously difficult, we used a combination of techniques to identify two systems with different effects on GBS pathogenesis. For one of the systems, we propose that fructose-6-phosphate, a metabolite in glycolysis, is sufficient to induce a regulatory response involving a sugar transport system. Our catalogue and classification of TCS may guide further studies into the role of TCS in GBS pathogenicity and biology.**

Received 20 March 2014 **Accepted** 10 April 2014 **Published** 20 May 2014

Citation Faralla C, Metruccio MM, De Chiara M, Mu R, Patras KA, Muzzi A, Grandi G, Margarit I, Doran KS, Janulczyk R. 2014. Analysis of two-component systems in group B *Streptococcus* shows that RgfAC and the novel FspSR modulate virulence and bacterial fitness. mBio 5(3):e00870-14. doi:10.1128/mBio.00870-14.

Invited Editor Victor Nizet, University of California, San Diego **Editor** Larry McDaniel, University of Mississippi Medical Center

Address correspondence to Robert Janulczyk, Robert.Janulczyk@novartis.com.

Streptococcus agalactiae, or group B *Streptococcus* (GBS), is a human pathogen that causes septicemia and meningitis in neonates (1, 2), and it is also a known cause of bovine mastitis (3). In this decade, GBS remains the dominant cause of infant morbidity and mortality in the United States (4), and it has also been recognized as an important cause of infections in immunocompromised patients and the elderly (5). GBS is a commensal in the rectovaginal tract of 20% to 30% of healthy women (6). However, by vertical transmission intrapartum, it may transition to an invasive pathogen, resulting in pneumonia, sepsis, and meningitis (7). The physiopathology of GBS infections implies that this bacterium encounters several very different microenvironments during colonization and the infectious process. The transition of the organism from a commensal niche (e.g., vaginal tract) to invasive niches (e.g., blood, lung, brain, and other organs) is likely to require adaptive changes, and a well-known way for bacteria to monitor and respond to their environment is by the use of two-component signal transduction systems (TCS).

TCS are typically organized in operons that encode a sensing histidine kinase (HK) and a response regulator (RR). The HK

harbors an N-terminal input domain that recognizes a specific stimulus. The information is then transduced through intramolecular conformational changes, resulting in the phosphorylation and activation of the C-terminal transmitter domain. This domain, in turn, activates its cognate receiver, encoded by the N-terminal domain of the RR. Once activated, the RR gives rise to an intracellular response through the C-terminal effector (or output) domain. This response typically results in differential gene expression. Sequence homology is generally a poor predictor of sensing mechanisms or specific stimuli, while domain architecture may provide clues that assist in assigning HKs to one of three groups: extracellular sensing, membrane sensing, and cytoplasmic sensing (8).

Overall, the role of TCS in GBS pathogenesis is not well understood. The most studied system is CovRS, an important regulator in *Streptococcus* spp. In GBS, the CovRS regulon extends to 7% to 27% of the genome (depending on growth conditions) and includes different functional categories, such as cell envelope, cellular processes, metabolism, and virulence factors (9–12). The RRs CiaR (13), Sak189 (14), and LiaR (15) are reported to directly influence *in vivo* virulence in GBS. Moreover, the TCS DltRS (16) and RgfAC (17, 18) have been shown to affect gene expression in GBS.

In the present study, we aimed to better understand the role of TCS in GBS pathophysiology by adopting a stepwise screening strategy. First, inventory, comparative genomics analysis, and sensing mechanism classification were performed through a bioinformatics approach. Second, by transcriptional analysis and identification of output domains related to virulence, we selected five systems for further study. We generated TCS knockout mutants and analyzed their transcriptome *in vitro*, as well as their contribution to virulence and colonization *in vivo*. One TCS was further characterized, and we propose evidence for a specific stimulus-response circuit.

RESULTS

Identification and comparative genomics of TCS. For the purposes of our study, we focused our main attention on serotype V GBS isolates. Type V is the most common capsular serotype associated with invasive infection in nonpregnant adults and has increased among neonatal invasive disease strains in recent years, accounting for approximately one-third of clinical isolates in the U.S. population (19). To identify possible TCS, genes predicted to encode HKs or RRs in the GBS type V strain 2603 V/R genome were collected from the P2CS database (http://www.p2cs.org) (20) and the loci were compared with those in a second type V genome (strain CJB111). A total of 38 genes (21 systems) were identified (Table 1). Seventeen of these loci contained a cognate pair of HK/RR-encoding genes, and an additional 4 TCS genes were orphans in strain 2603 V/R, while the corresponding numbers of cognate pairs and orphans in strain CJB111 were 19 and 2, respectively. Each TCS locus, whether paired or orphaned, was assigned a number in order of its appearance on the chromosome. The predicted TCS proteins were then used as queries to identify corresponding gene loci in 251 other GBS genomes (draft and complete), representing isolates from different host species (predominantly human and bovine). Overall, the 21 TCS were very well conserved (>98% identity) across the genomes. Our analysis was unidirectional, and we do not exclude the presence of additional TCS. We have likely underestimated the number of fully functional orthologous systems, due to a number of TCS sequences being located in the vicinity of contig breaks. With the very limited variability observed in a large set of genomes, the TCS identified here appear to be part of the GBS core genome. TCS-17 (also known as RgfAC) presented an interesting case of variability. While TCS-17/RgfAC is complete and conserved in 64 strains, 118 strains have an orphan TCS-17/RgfAC where only the RR/RgfA is present, and another 61 strains had polymorphisms that inactivated the RR/RgfA. Moreover, orphaned and complete loci may represent two distinct families. While the protein sequence conservation is typically high (99% identity) when comparing RRs within a family (e.g., orphaned versus orphaned), a similar comparison across families shows a decreased sequence conservation (79% identity). Genomes with an orphan TCS-17 may have undergone recombinatorial events, as they show larger deletions in the locus with short remnants of putative *hk* or *rr* genes.

A minimum spanning tree (MST) using the 40 TCS genes and all their respective variants was created to identify potential TCS profile clusters (Fig. 1). Interestingly, bovine isolates appeared to contain TCS profiles that clustered together and were relatively more distant from human isolates. TCS-17 again constituted a particular example in which RR variants appeared to group according to the host species from which they were isolated (see Fig. S1 in the supplemental material). Variant 2 was found in 43% of bovine strains versus 6% of human strains. Conversely, variant 4 was found in 41% of human strains and only 13% of bovine strains.

Domain architecture for TCS in the genome of CJB111. For further experimental analysis, we shifted our focus to the serotype V strain CJB111, which is more virulent than 2603 V/R in mouse models and for which a custom microarray was available in-house. The CJB111 TCS gene identifiers are listed in Table 1. We analyzed the domain architecture of all the HK proteins in the genome of CJB111 and predicted the mechanism of stimulus perception according to criteria reported in the literature (8) (Fig. 2). Nine of the HKs contained an N-terminal domain with two transmembrane helices with a spacer of 50 to 300 amino acids, typical for extracellular (EX) sensing. Eight HKs contained 2 to 6 predicted transmembrane-spanning regions separated by short spacers and were predicted to be membrane sensing (TM). Only one HK was classified as cytoplasmic (C) sensing.

We also observed that all the RR proteins had a DNA binding output domain, indicating a role as direct transcriptional regulators. Interestingly, the LytTR output domain was the second most common output domain in GBS (15%), while it accounts for a smaller percentage (4%) in prokaryotes in general. LytTR-type output domains have been noted for the control of virulence factors in several important bacterial pathogens (20).

Transcriptional analysis of TCS. Transcriptional analysis was performed in early logarithmic (EL) and early stationary (ES) phase using a custom microarray chip designed on the CJB111 genome. We noted that several TCS were significantly upregulated in ES phase, and 3 of these (TCS-2, TCS-16, and TCS-21) were upregulated 4-fold or more. As many TCS respond to stress conditions like those encountered in stationary phase (lack of nutrients, low pH, and accumulation of toxic metabolites), we hypothesized that these systems could be involved in bacterial stress responses and selected them as targets for mutagenesis. To further understand the levels of expression of each selected TCS during bacterial growth *in vitro*, we measured the gene transcripts of the

TABLE 1 Comparative genomics of TCS

TCS locus	Locus tag in 2603 V/R	Type	No. of strains with: Ortholog: Present[a]	Absent[b]	Stop[c]	No. of proteins with: Ambiguity[d]	Variance[e]	Avg % identity (SD)	JCVI designation[f]	Gene name(s) (reference)[g]
1	SAG0123	RR	240	4	0	9	6	99.02 (0.46)	SAM0116	
	SAG0124	HK	246	3	0	4	17	98.61 (0.58)	SAM0117	
2	SAG0182	HK	240	3	6	4	21	99.53 (0.22)	SAM0183	
	SAG0183	RR	248	3	1	1	6	99.06 (0.48)	SAM0184	
3 (orphan)	SAG0310	HK	198	3	12	40	27	98.17 (3.32)	SAM0322	
			246	3	2	2	30	97.87 (2.39)	SAM0323	
4	SAG0321	HK	250	3	0	0	9	99.28 (0.29)	SAM0333	*liaSR* (15)
	SAG0322	RR	248	3	0	2	4	99.30 (0.25)	SAM0334	
5	SAG0393	RR	242	10	0	1	4	99.13 (0.39)	SAM0401	
	SAG0394	HK	239	3	1	10	11	99.36 (0.28)	SAM0402	
6	SAG0616	RR	226	26	0	1	2	99.54 (0.00)	SAM0583	*sak188*/*sak189*
	SAG0617	HK	209	25	4	15	11	97.23 (4.53)	SAM0584	(14)
7 (orphan)	SAG0712	RR	240	2	1	10	7	99.11 (0.38)	SAM0733	
8	SAG0719	RR	241	4	7	1	7	99.28 (0.19)	SAM0741	
	SAG0720	HK	247	4	1	1	16	99.53 (0.13)	SAM0742	
9	SAG0976	RR	237	4	9	3	12	98.86 (0.56)	SAM0983	
	SAG0977	HK	247	4	0	2	12	99.04 (0.41)	SAM0984	
10	SAG0984	HK	250	3	0	0	20	99.47 (0.18)	SAM0991	*ciaRH* (13)
	SAG0985	RR	250	3	0	0	4	99.34 (0.24)	SAM0992	
11	SAG1016	RR	248	3	1	1	14	98.91 (0.45)	SAM1027	
	SAG1017	HK	244	3	1	5	25	99.12 (0.39)	SAM1028	
12	SAG1327	HK	249	3	0	1	15	99.27 (0.27)	SAM1289	
	SAG1328	RR	248	3	1	1	10	98.80 (0.65)	SAM1290	
13	SAG1624	HK	249	1	1	2	27	99.35 (0.38)	SAM1583	*covRS* (10)
	SAG1625	RR	252	1	0	0	6	99.19 (0.32)	SAM1584	
14	SAG1791	HK	244	0	3	6	17	99.34 (0.23)	SAM1775	*dltRS* (16)
	SAG1792	RR	232	1	17	3	15	98.70 (0.54)	SAM1776	
15 (orphan)	SAG1922	RR	239	5	6	3	8	99.54 (0.30)	SAM1860	
16	SAG1946	RR	248	3	1	1	16	99.11 (0.28)	SAM1885	
	SAG1947	HK	245	3	3	2	27	99.12 (0.39)	SAM1886	
17 (orphan)			123	128	0	2	8	88.26 (10.33)	SAM1896	*rgfAC* (17)
	SAG1957	RR	182	3	61	7	12	98.71 (0.72)	SAM1897	
18	SAG1960	HK	246	4	2	1	23	99.10 (0.46)	SAM1900	
	SAG1961	RR	239	4	0	10	12	98.92 (0.42)	SAM1901	
19	SAG2054	RR	249	2	1	1	15	98.69 (0.60)	SAM1962	
	SAG2055	HK	237	2	7	7	21	99.14 (0.36)	SAM1963	
20	SAG2122	RR	237	14	0	2	14	98.85 (0.42)	SAM2038	
	SAG2123	HK	236	13	2	2	19	98.87 (0.61)	SAM2039	
21	SAG2127	HK	228	21	0	4	15	99.26 (0.30)	SAM2043	
	SAG2128	RR	223	12	6	12	3	99.52 (0.21)	SAM2044	

[a] Strains with putatively functional ortholog (i.e., >75% identity for at least 90% of the query sequence).
[b] Strains where no ortholog was identified.
[c] Strains where proteins were truncated and possibly inactivated.
[d] Proteins with nucleotide ambiguities or proximity to contig break.
[e] Distinct variant proteins.
[f] J. Craig Venter Institute (formerly TIGR) gene names of *hk* and *rr* genes in the CJB111 strain used in the experimental studies.
[g] Previously reported gene name and citation.

HKs at four time points (representing early, mid-, and late logarithmic and early stationary phases) using a real-time quantitative (qRT)-PCR analysis (see Fig. S2 in the supplemental material). These data confirmed that TCS-2, TCS-16, and TCS-21 are upregulated only in ES phase.

Transcriptional regulators with the LytTR-type output domains control the production of virulence factors in several important bacterial pathogens (20). We therefore selected as mutagenesis targets the three TCS containing an RR with a LytTR-type DNA binding domain, i.e., TCS-2 (upregulated at ES phase), TCS-11, and TCS-17/RgfAC. Thus, a total of five TCS exhibiting either the presence of a LytTR domain and/or upregulation during ES were selected for further experimentation (Table 2).

Expression microarray analysis of TCS mutants. The 5 selected TCS loci were modified genetically by in-frame deletion of the genes encoding RRs. There were no apparent differences in colony size, hemolysis, or other macroscopic features between the wild-type (WT) strain and the five isogenic mutant strains on blood agar or tryptic soy agar plates (data not shown). Mutant strains grown in complex medium exhibited growth curves identical to that of the wild-type parental strain (see Fig. S3 in the supplemental material).

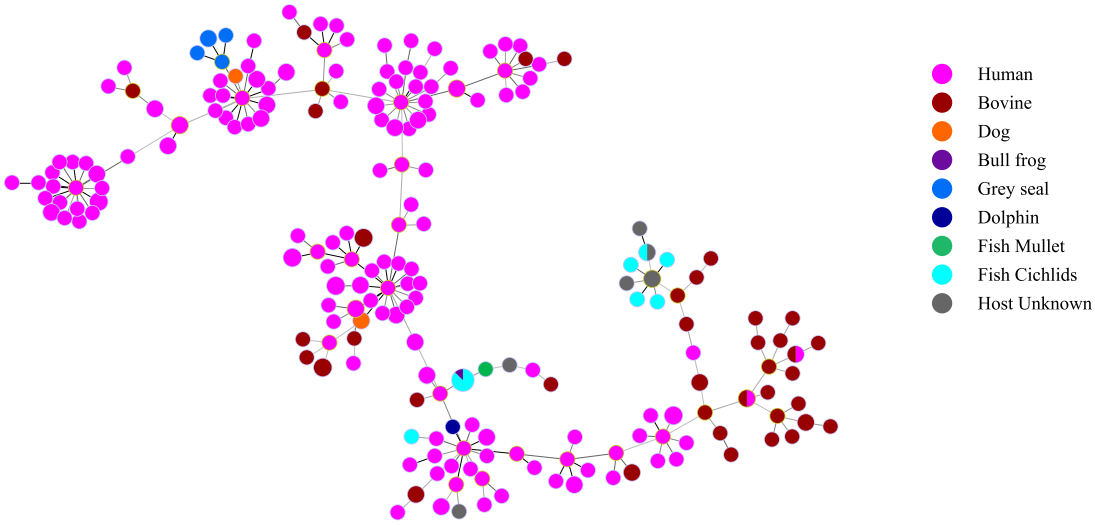

FIG 1 Minimum spanning tree (MST), obtained using the goeBurst algorithm and based on the TCS protein similarity in 253 GBS genomes. Isolates are from different hosts, as indicated, and each node represents a TCS profile. The sizes of the nodes are proportional to the numbers of isolates with each profile.

Global transcriptional analysis was performed by microarray technology. Gene expression of all of the predicted genes (n = 2,232) in the CJB111 genome was performed by comparing the WT strain with each of the five mutant strains in ES phase (Fig. 3A). Experimental design, chip validation, quality control, and data analysis were performed as described in Materials and Methods. Further validation of the microarray data was performed by qRT-PCR, using probes for 9 independent transcriptional units (see Fig. S4 in the supplemental material). Overall, all five mutants exhibited differential transcription of genes in comparison to the gene transcription in the wild type when using a permissive threshold (±2-fold change and a P value of <0.05). The number of regulated genes ranged from 2 (Δ*rr17* strain; see Materials and Methods) to 66 (Δ*rr11* strain). Two mutants (the Δ*rr11* and Δ*rr21* strains) showed predominantly downregulated genes, suggesting that these RRs act as activators. We observed that some genes appeared to be regulated in two or more independent mutant strains (Fig. 3B). In particular, 20 genes were regulated in both the Δ*rr21* and the Δ*rr11* strain (19 genes downregulated and 1 gene upregulated in both strains).

A more stringent threshold was applied to identify the most highly regulated genes (±4-fold change and a P value of <0.05). Three mutants (Δ*rr2*, Δ*rr11*, and Δ*rr16* strains) showed a total of 18 highly regulated genes, and in two of them, such genes were identified adjacent to the TCS locus (Table 3). In particular, the Δ*rr2* mutant exhibited downregulation of SAM0185 and SAM0186, encoding two proteins similar to LrgAB in *Streptococcus mutans*. In this species, LrgAB is reported to be under the control of an adjacent TCS (homologous to TCS-2) and was suggested to have a role in the control of virulence and biofilm formation (21, 22). The Δ*rr16* mutant showed strong downregulation of an adjacent phosphotransferase system (PTS) and concomitant upregulation of another PTS system in a different locus. All of the highly regulated genes were subjected to confirmation by qRT-PCR, using one probe set per transcriptional unit (Table 3). Moreover, qRT-PCR experiments were repeated on chromosomally complemented strains where the deleted *rr* gene was replaced with the WT form, which confirmed that the WT phenotype was restored (Table 3).

Phenotype microarray screening shows that TCS-16 influences carbon source utilization. Our microarray analysis showed differential regulation of two different PTS (SAM1715 to SAM1716 and SAM1887 to SAM1890) in the Δ*rr16* mutant strain, suggesting a possible involvement in the monitoring of carbon source availability. The WT and Δ*rr16* strains were grown on 192 different single carbon sources using the phenotype microarray (PM) technology (see Fig. S5 in the supplemental material). One compound showed a clear difference between the WT and mutant strain. The WT strain exhibited growth comparable to that of the positive control when supplied with fructose-6-phosphate (Fru-6-P), while the Δ*rr16* strain showed no growth. The experiment was repeated using the complemented (knock-in [KI]) KI*rr16* strain, which showed a growth profile indistinguishable from that of the WT strain (Fig. S5).

To confirm this phenotype in an independent system and to understand if it could be extended to other hexose-6-phosphate sugars, we used a chemically defined medium (CDM) (23) where glucose, fructose, mannose, or the corresponding hexose-6-phosphate counterpart of each was used as the primary carbon source (Fig. 4). The WT, Δ*rr16*, and KI*rr16* strains grew well on glucose, fructose, and mannose, while only the WT and KI*rr16* strains grew on Fru-6-P. The other phospho-sugars did not allow any bacterial growth. We concluded that TCS-16 is necessary for the growth of strain CJB111 on Fru-6-P as the primary carbon source.

TCS-16 gene regulation in response to extracellular Fru-6-P. We subsequently investigated the impact of Fru-6-P on the transcription of TCS-16 and its adjacent PTS system by using qRT-PCR. Bacteria grown in CDM were subjected to a substitution of glucose for Fru-6-P upon entry into mid-logarithmic phase (see Materials and Methods). Compared to its transcription in bacteria exposed to glucose, the transcription of the *hk16* gene increased 22-fold when bacteria were exposed to Fru-6-P (Fig. 5A). This response was observed in the WT, absent in the Δ*rr16* strain, and

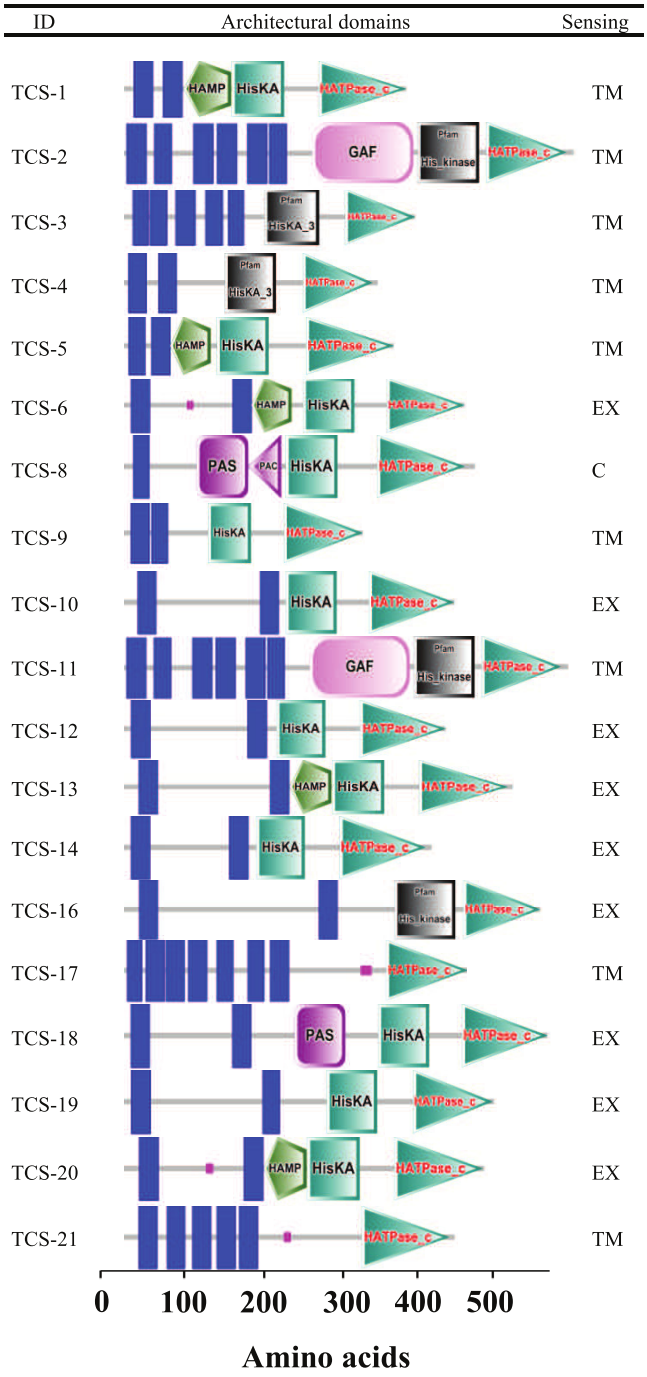

FIG 2 Domain architecture of histidine kinases. Protein sequences were analyzed using SMART http://smart.embl-heidelberg.de, and PFAM domains were included. The scale bar shows the sequence length in amino acids. Blue vertical bars represent putative transmembrane helices, and pink squares represent low-complexity regions. Various functional domains are indicated by the remaining colored elements and using the SMART nomenclature (e.g., GAF, PAS, HAMP, PAC). The SMART HATPase_c domain in TCS-17/RgfAC is an outlier homolog and was found by using the schnipsel database. Sensing mechanisms were manually predicted as transmembrane (TM), extracellular (EX), and cytoplasmic (C).

partially restored in the complemented KI*rr16* strain. Concomitantly (Fig. 5B and C), a similar pattern was observed for the adjacent PTS system (3,000-fold upregulation) and for the SAM1402 gene (2.5-fold upregulation), a putative hexose-6-P transporter gene that we identified in the genome of CJB111. A downregulation of the SAM1402 gene (1.5-fold) in the Δ*rr16* strain was also observed in the microarray.

TABLE 2 CJB111 expression of selected TCS

TCS locus	Locus tag	Type	Fold change[a]	*P* value[b]
2	SAM0183	HK	6.1	7.4×10^{-4}
	SAM0184	RR[c]	5.6	6.0×10^{-3}
11	SAM1027	RR[c]	0.9	NS
	SAM1028	HK	1.5	NS
16	SAM1885	RR	4.5	3.8×10^{-3}
	SAM1886	HK	5.5	1.1×10^{-3}
17	SAM1896	HK	1.1	NS
	SAM1897	RR[c]	1.6	NS
21	SAM2043	HK	37.0	6.0×10^{-8}
	SAM2044	RR	19.5	6.3×10^{-5}

[a] Relative expression of the TCS in ES compared to EL growth phase.
[b] NS, the fold change was considered not significant if the *P* value was >0.05.
[c] Contains a LytTR output domain.

Fru-6-P is an intracellular metabolic intermediary of the glycolytic pathway. Bacterial lysis constitutes a possible scenario where Fru-6-P would be found in the extracellular space. We wanted to investigate whether TCS16 would respond under such conditions. Bacteria were grown in CDM until mid-logarithmic phase, and the medium was changed to CDM without glucose in the presence or absence of bacterial lysate (see Materials and Methods). The transcriptional levels of TCS-16, its adjacent PTS system, and the putative hexose-6-P transporter were then analyzed by qRT-PCR. The *hk16* gene transcription increased 10-fold when bacteria were exposed to bacterial lysate compared to its transcription in the control (Fig. 5D). Concomitantly, an upregulation of the PTS system (200-fold) and the SAM1402 gene (5-fold) was observed (Fig. 5E and F). These responses were absent in the Δ*rr16* strain and totally restored in the complemented KI*rr16* strain.

TCS-16 influences vaginal persistence in mice. In a recent work, carbon catabolite repression in *Streptococcus pyogenes* was shown to influence asymptomatic colonization of the murine vaginal mucosa, suggesting that the availability of carbon sources may be subject to monitoring by the bacteria (24). We subsequently investigated whether TCS-16 could play a role in bacterial survival during colonization, utilizing the Δ*rr16* mutant strain in a mouse model of GBS vaginal colonization (25, 26). CD-1 mice in estrus were inoculated with ~1×10^7 CFU in the vaginal lumen and, on successive days, bacteria were recovered by swabbing and quantified by serial dilution and plating on selective medium. Interestingly, the Δ*rr16* mutant exhibited decreased persistence in the vaginal tract (Fig. 6). The statistically significant differences were observed at later time points during the experiment ($P = 0.004$, day 5; $P = 0.02$, day 7) and suggested a gradual decline in colonization with the mutant strain, while the WT remained relatively stable throughout the experiment. Identical experiments were performed with the remaining mutant strains, and the results were similar to those with the WT strain, underlining that the phenotype seen in the Δ*rr16* mutant was unique among the strains tested.

TCS-17/RgfAC influences virulence in a murine model of systemic infection. To further investigate the role of the selected

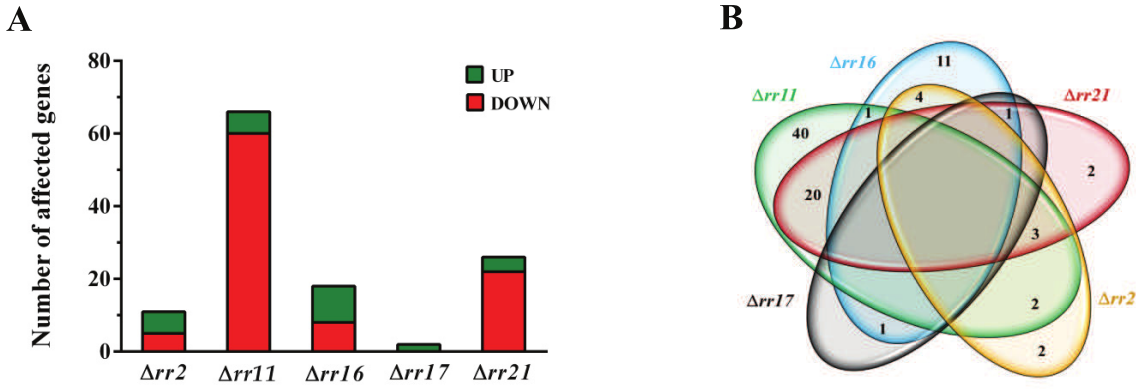

FIG 3 Microarray analysis of TCS mutant strains. (A) Bars represent the numbers of genes up- or downregulated in early stationary (ES) phase compared to their transcription in the WT strain. The threshold used is ±2-fold change and a *P* value of ≤0.05. (B) Venn diagram showing overlaps of gene regulation between the mutants. The fields show the number of individual genes significantly regulated in single or multiple mutant strains.

TCS in GBS pathogenesis, we compared the relative levels of virulence of CJB111 and the Δ*rr* mutants using an *in vivo* mouse model of infection (27, 28). CD-1 mice were infected intravenously with 1.5×10^7 CFU of the WT or mutant strains. Bacteremia was confirmed in all mice by counting viable cells in blood samples collected 24 h postinfection, and there was no significant difference in bacterial loads between the WT and mutant strains (data not shown). Over the course of infection, animals were sacrificed at individual endpoints (when moribund) or upon termination of the experiments, and blood, brain, and lung tissues were collected for bacterial counts. Overall, the only mutant strain with a virulence phenotype was the Δ*rr17* strain, infection with which exhibited a significantly higher mortality than was observed during infection with the WT strain ($P = 0.003$, log-rank test) (Fig. 7A). Interestingly, no significant differences were observed in bacterial loads in brain, blood, and lung tissues when comparing the WT and Δ*rr17* strains (Fig. 7B to D). Blood and brain tissues from mice infected with the Δ*rr17* strain contained more individual samples with very high bacterial counts, but such samples were exclusively from moribund mice (Fig. 7B and C). None of the other mutant strains showed an appreciable difference from the WT strain (data not shown).

DISCUSSION

In the present study, we conducted genome-wide inventory, classification, and comparative genomics of TCS in GBS and concluded that they are highly conserved and part of the core genome. Nonetheless, the profile of TCS allelic variants differed somewhat when comparing human GBS isolates with those from bovine and other hosts. In our classification of sensing mechanisms, only one HK was classified as cytoplasmic sensing, while this is typically a more frequent category (8). A comparison of the number of TCS (corrected for genome size) in various pathogenic and nonpathogenic *Lactobacillales* spp. was also performed. In the nine species

TABLE 3 Highly regulated genes in early stationary phase

Mutation	Locus tag	Annotation	Gene	Fold change in microarray	*P* value[a]	KO strain/KI strain fold changes in qRT-PCR[b]
Δ*rr2*	SAM0185	LrgA family subfamily, putative	*lrgA*	−11.5	4.0×10^{-5}	−6.14/−1.18
	SAM0186	LrgB family protein	*lrgB*	−8.8	1.2×10^{-4}	
Δ*rr11*	SAM0011	Phosphoribosylformyl-glycinamidine synthase		−4.0	2.2×10^{-4}	
	SAM0012	Amidophosphoribosyl-transferase	*purF*	−4.0	3.0×10^{-3}	−2.23/+2.98
	SAM0013	Phosphoribosylformyl-glycinamidine cycloligase	*purM*	−4.3	2.4×10^{-4}	
	SAM0014	Phosphoribosylglycinamide formyltransferase	*purN*	−4.3	1.8×10^{-3}	
	SAM0064	Ribosomal protein S5	*rpsE*	−4.4	1.8×10^{-5}	−2.01/+1.56
	SAM1026	Carbon starvation protein, putative	*cstA*	−5.7	1.6×10^{-5}	−10.95/+2.11
	SAM1057	Conserved hypothetical protein		−5.1	1.8×10^{-5}	
	SAM1058	Conserved hypothetical protein		−5.2	5.8×10^{-7}	
	SAM1059	Carbamoyl-phosphate synthase, large subunit	*carB*	−7.4	3.0×10^{-7}	−4.72/−1.69
	SAM1060	Carbamoyl-phosphate synthase, small subunit	*carA*	−4.2	4.2×10^{-2}	
Δ*rr16*	SAM1715	PTS system, IIC component	*fruA-2*	+4.0	1.4×10^{-4}	+3.25/−1.06
	SAM1716	PTS system, IIA component	*fruA-2*	+4.1	2.6×10^{-4}	
	SAM1887	PTS system, IID component		−31.6	1.6×10^{-7}	−324.0/+1.72
	SAM1888	PTS system, IIC component		−72.0	1.0×10^{-7}	
	SAM1889	PTS system, IIB component		−55.7	1.0×10^{-6}	−6.14/−1.18
	SAM1890	PTS system, IIA component, putative		−52.0	1.8×10^{-7}	

[a] Inclusion threshold is a *P* value of ≤0.05 and fold change of ±4 compared to the WT strain).
[b] Fold changes in knockout/complemented strains compared to the WT strain.

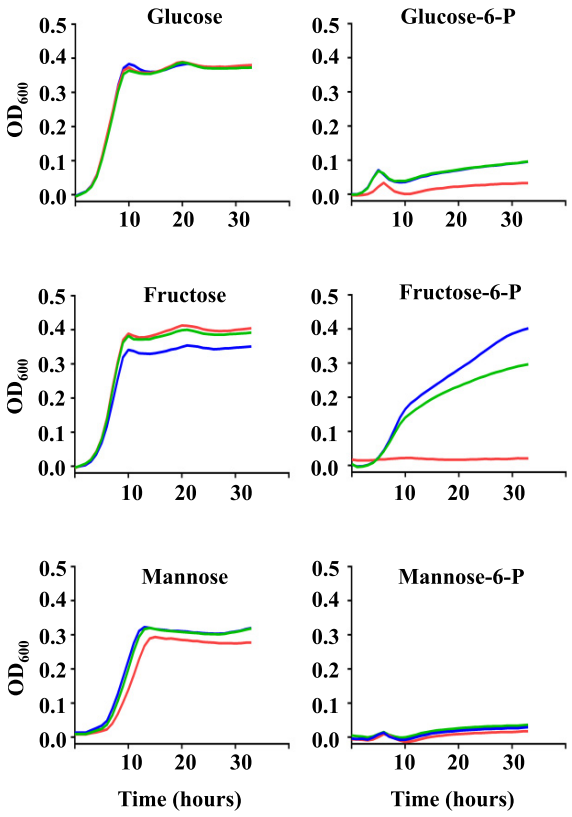

FIG 4 Growth curves of WT (blue), Δ*rr16* (red), and KI*rr16* (green) strains in CDM supplemented with 10 mg/ml of glucose or glucose-6-phosphate, fructose or fructose-6-phosphate, or mannose or mannose-6-phosphate. Growth curves are from triplicate samples, and the background (negative control, no sugar added) was subtracted.

examined, GBS and *S. pyogenes* showed the highest frequencies of TCS, with medians of 38 and 36 TCS components, respectively (data not shown), compared to a typical range of 15 to 32 for the other *Lactobacillales*. This suggests that the two pathogens may require particular fine tuning of transcription in response to changing environments.

Transcriptome analysis was performed on five selected systems, and we observed a limited number of genes that were highly regulated for three TCS. TCS-2 regulates the adjacent *lrgAB* operon, similar to what has been described for *S. mutans* (22). TCS-11 regulates genes involved in purine metabolism and carbon starvation. TCS-16 highly regulates two PTS operons and is discussed in more detail below.

TCS-17/RgfAC has already been described in GBS strain O90-R, where it negatively regulates the transcription of C5a peptidase (*scpB*), a known virulence factor (17). Moreover, an independent group demonstrated that in clonal complex 17 (CC17) strains, RgfAC negatively regulates the *fbsA* gene, encoding fibrinogen binding proteins (18). FbsA may have a role in protecting the bacteria against opsonophagocytosis, promoting adhesion to lung epithelial cells, and increasing survival in human blood (29, 30). We did not observe any upregulation of the above-described genes in the Δ*rr17* strain, which may be due to differences in the experimental protocol (time points) or in the genetic background (CJB111 belongs to CC1 [31]). Nonetheless, the Δ*rr17* strain was hypervirulent in our murine model of systemic infection, consistent with a potential upregulation of virulence factors in the absence of this transcriptional regulator. TCS-17 was also the only system where specific allelic variants were distributed differently between human and bovine isolates, suggesting a potential host-specific role during infection.

The second system of particular interest was TCS-16. Transcriptome analysis showed prominent downregulation of an adjacent operon that encodes a putative PTS (Man/Fru/Sor family) and concomitant upregulation of another PTS (Fru family). TCS-16 was classified as an extracellular sensing system, and we hypothesized that it may be involved in monitoring and responding to the availability of nutrients (8). When bacteria were subjected to a large variety of different carbon sources in chemically defined medium, one compound, Fru-6-P, resulted in a complete growth defect, which was fully restored when the Δ*rr16* mutation was complemented. Further experiments *in vitro*, using phosphorylated and nonphosphorylated hexose sugars, confirmed these results. We thus conclude that a functional TCS-16 is necessary for growth on Fru-6-P. Investigation of the transcriptional events in the locus showed that, upon exposure to extracellular Fru-6-P, there is induction of TCS-16 and a concomitant drastic upregulation of the adjacent PTS operon. As the Δ*rr16* strain showed no such response, while the complemented strain exhibited a partial restoration, we conclude that a functional TCS-16 is necessary for autoinduction and regulation of the adjacent PTS operon. We propose that extracellular Fru-6-P is a signal for TCS-16 and that the gene locus be named *fspSR*, for fructose-six-phosphate sensor histidine kinase and response regulator. Despite the magnitude of the influence on PTS transcription, the growth defect observed in the Δ*rr16* (Δ*fspR*) strain is difficult to explain in terms of a direct link between the upregulated PTS and the utilization of Fru-6-P as an energy source. To our knowledge, PTS-dependent import of phosphorylated sugars has not been described. However, other such uptake mechanisms are known, and UhpT (major facilitator superfamily) in *Escherichia coli* represents an example where the controlling TCS (UhpAB) is necessary for the growth of *E. coli* upon Glc-6-P and Fru-6-P (32, 33). We identified a homologue of UhpT in the genome of CJB111 (SAM1402), and analysis of the protein suggests it could function as a hexose-6-P transporter (http://www.tcdb.org/). SAM1402 was among the genes significantly downregulated in the Δ*rr16* (Δ*fspR*) mutant transcriptome, and subsequent experiments confirmed that TCS-16/FspSR upregulates the SAM1402 gene in response to extracellular Fru-6-P. The biological relevance of our link between Fru-6-P and TCS-16/FspSR is difficult to ascertain, as the availability of Fru-6-P in the extracellular milieu is presumably limited or unknown. Nevertheless, our *in vivo* screening showed reduced vaginal persistence of the Δ*rr16* (Δ*fspR*) strain in mice. The PTS and associated carbon metabolism pathways may have an impact on *in vivo* fitness and virulence, as previously demonstrated for several different pathogens (34–38). One possibility is that Fru-6-P may be released from dying microorganisms in the complex microbiota of the vagina or in stationary-phase *in vitro* cultures, and GBS could consequently initiate a scavenging response involving upregulation of sugar transporters. This hypothesis was supported by our data showing that there is an induction of the TCS-16 response upon exposure to bacterial lysate. This response was observed in the WT and complemented strains but not in the Δ*rr16* (Δ*fspR*) strain, confirming that a functional TCS-16 is nec-

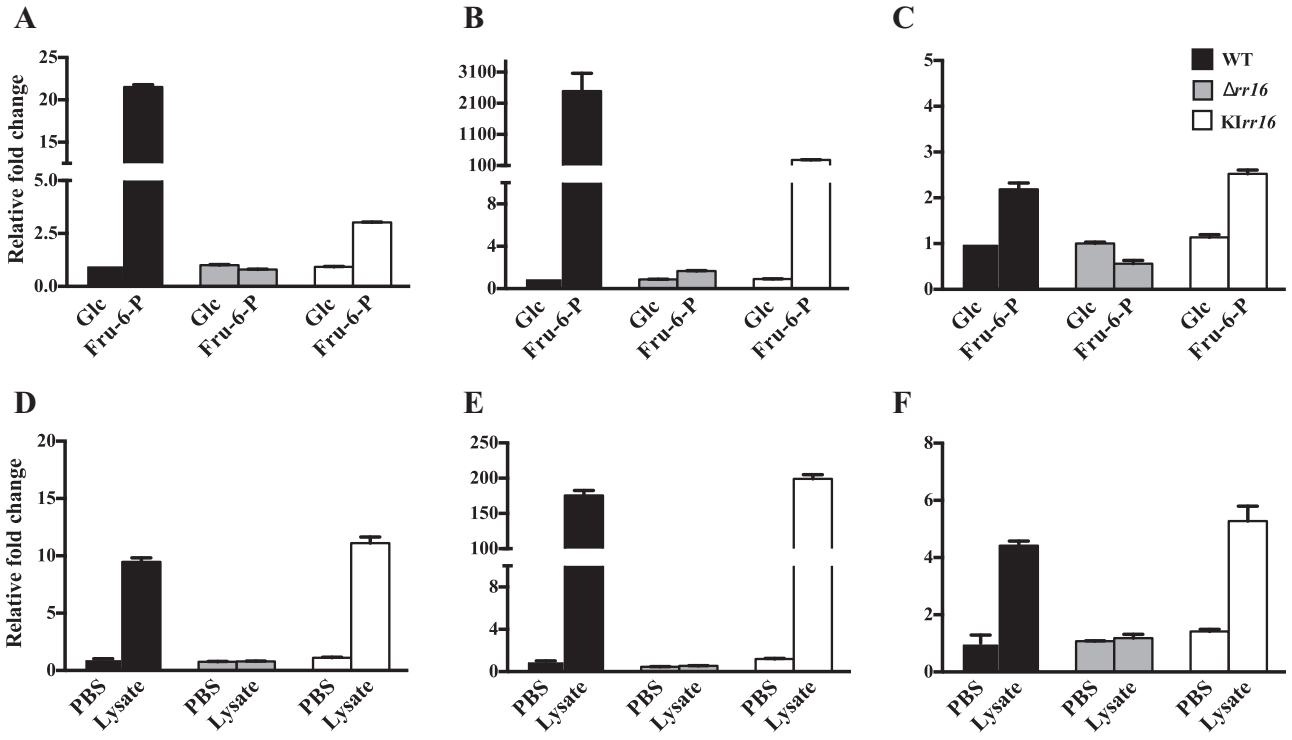

FIG 5 Results of qRT-PCR with probes for SAM1885 (HK) (A, D), SAM1888 (PTS, IIC component) (B, E), and SAM1402 (putative hexose-phosphate transporter) (C, F) using RNA extracted from WT, Δ*rr16*, and KI*rr16* strains. (A to C) Bacteria grown in CDM were subjected to a pulse of either glucose (Glc) or fructose-6-phosphate (Fru-6-P) as the main carbon source for 30 min prior to RNA extraction. Bars represent gene expression when exposed to Fru-6-P relative to gene expression during growth in glucose. (D to F) Bacteria grown in CDM were subjected to a pulse of PBS or bacterial lysate for 30 min prior to RNA extraction. Bars represent gene expression when cells were exposed to bacterial lysate relative to gene expression in the PBS control. The experiment was performed twice. Bars represent technical triplicates, and error bars show the standard errors of the means.

essary to upregulate sugar transporters in the presence of lysed GBS components. Moreover, in a previous work using a different strain, the PTS operon described above, together with several other PTS, were highly downregulated under high-glucose conditions, supporting a role for this and similar systems under conditions where nutrients are relatively scarce (12). Another speculative possibility is that FspSR may be activated upon entry/invasion of eukaryotic cells, through the presence of Fru-6-P as a central metabolite in glycolysis.

We have listed and classified TCS in GBS for further study and conclude that these TCS are very well-conserved intraspecies but with allelic profiles that vary somewhat according to the host. Our results provide new insights into four previously unknown TCS but also provide the first *in vivo* data supporting a role for RgfAC in virulence. Finally we identified FspRS, a new TCS that is involved in vaginal persistence and responds to fructose-6-phosphate by the upregulation of genes involved in sugar transport.

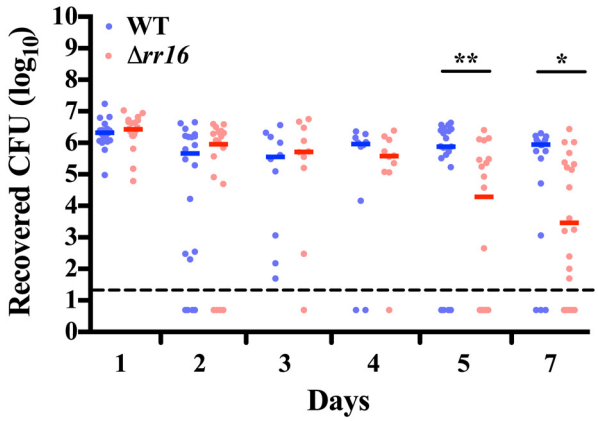

FIG 6 Murine vaginal colonization model. The vaginal lumen of CD-1 mice was inoculated with 10^7 CFU of WT or Δ*rr16* bacteria, and bacterial persistence was determined by counting viable cells. Results shown are from two independent experiments. The detection limit is represented by the dashed line. Horizontal bars represent medians, and the Mann-Whitney *U* test was used for statistical analysis. *, $P < 0.05$; **, $P < 0.005$.

MATERIALS AND METHODS

Bacterial strains and growth conditions. GBS strain CJB111 (Carol Baker Collection, Division of Infectious Diseases, Baylor College of Medicine, Houston, TX) and its isogenic derivatives were grown in Todd-Hewitt broth (THB medium; Difco Laboratories) at 37°C, 5% CO_2. Tryptic soy broth (Difco Laboratories) with 15 g/liter agar (TSA) was used as the solid medium. Max Efficiency DH5α competent *E. coli* cells (Invitrogen) were used for transformation, propagation, and preparation of plasmids. *E. coli* was grown at 37°C with agitation (180 rpm) in Luria-Bertani (LB; Difco Laboratories) broth or on 15 g/liter agar plates (LBA). Erythromycin (Erm) was used for selection of GBS (1 μg/ml) or *E. coli* (100 μg/ml) cells containing the pJRS233-derived plasmids used for mutagenesis (see below).

Strains CJB111, CJB111Δ*rr16*, and CJB111KI*rr16* were also grown in chemically defined medium (CDM) (23) or in CDM where glucose was replaced with 10 g/liter glucose-6-phosphate, fructose, fructose-6-

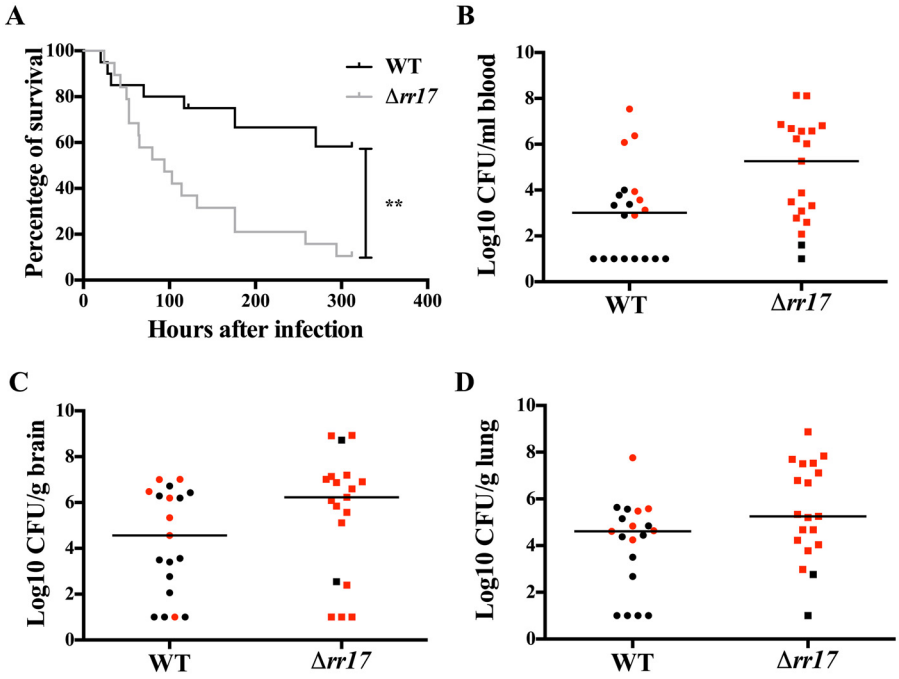

FIG 7 Murine intravenous challenge model. (A) Kaplan-Meyer survival plot of mice infected with 1.5×10^7 CFU of bacteria. The log-rank test was used for statistical analysis. (B to D) Bacterial counts (CFU) in blood, brain, and lung tissues from individual mice. Horizontal bars represent medians. Mice were euthanized when moribund (red) or at the end of the experiment (black).

phosphate, mannose, or mannose-6-phosphate (Sigma). Briefly, bacteria grown on THB plates were suspended in 5 ml of phosphate-buffered saline (PBS) until the optical density at 600 nm (OD_{600}) reached 0.3. Samples were then diluted 1:10 in PBS, and 88 μl of bacteria was added to 1.2 ml of medium with or without different carbon sources. Bacteria were grown in 96-well plates with 200 μl per well for 48 h at 37°C, and the OD_{600} was monitored automatically every 20 min in an automated reader (Sunrise; Tecan).

Construction of TCS isogenic mutants. To construct the knockout strains, a pJRS233 shuttle vector (39) containing each TCS locus with an in-frame deletion in the response regulator gene (*rr*) was constructed using a splicing by overlap extension PCR (SOEing-PCR) strategy (see Table S1 in the supplemental material) (40). Briefly, the up- and downstream regions of an *rr* gene were produced from CJB111 genomic DNA and then joined. The resulting fragment was cloned into pJRS233 using BamHI and XhoI restriction sites.

Five plasmids, pJRS233Δ*rr2*, pJRS233Δ*rr11*, pJRS233Δ*rr16*, pJRS233Δ*rr17*, and pJRS233Δ*rr21*, were obtained, each containing an insert with 700 to 800 bp upstream and downstream from the in-frame-deleted *rr* gene. The CJB111 genes thus inactivated were SAM0184 (*rr2*), SAM1027 (*rr11*), SAM1885 (*rr16*), SAM1897 (*rr17*), and SAM2044 (*rr21*).

To construct the respective chromosomally complemented knock-in (KI) strains, each wild-type locus was amplified and cloned into pJRS233 using BamHI and XhoI restriction sites (see Table S1 in the supplemental material). These plasmids were designated pJRS233KI*rr2*, pJRS233KI*rr11*, pJRS233KI*rr16*, pJRS233KI*rr17*, and pJRS233KI*rr21*.

An insertion/duplication and excision mutagenesis strategy was used to obtain either the in-frame deletions in the response regulator genes or the chromosomal replacements in the knockout mutants. In brief, pJRS233Δ*rr2*, -Δ*rr11*, -Δ*rr16*, -Δ*rr17*, and -Δ*rr21* plasmids purified from *E. coli* were used to transform CJB111 by electroporation, as previously described (41), except that we used M9 medium without glycine and Casamino acids. Transformants were selected by growth on TSA containing Erm at 30°C for 48 h. Integration was performed by growth of transformants at 37°C (nonpermissive temperature for the suicide shuttle vector) with Erm selection. Excision of the integrated plasmid was performed by serial passages in THB at 30°C and parallel screening for Erm-sensitive colonies on plates. Mutants were verified by PCR sequencing of the TCS loci. We obtained thus five knockout strains, each having had the response regulator gene of a specific TCS inactivated, which we designated CJB111Δ*rr2*, CJB111Δ*rr11*, CJB111Δ*rr16*, CJB111Δ*rr17*, and CJB111Δ*rr21*, abbreviated herein as the Δ*rr2* strain, Δ*rr11* strain, etc.

To obtain the chromosomally complemented strains, plasmids PJRS233KI*rr2*, -KI*rr11*, -KI*rr16*, -KI*rr17*, and -KI*rr21* were purified from *E. coli* and complementation of the respective mutant strains was performed as described above. The result was replacement of the deleted *rr* gene with the WT form. The complemented strains were designated CJB111KI*rr2*, CJB111KI*rr11*, CJB111KI*rr16*, CJB111KI*rr17*, and CJB111KI*rr21*, abbreviated herein as the KIΔ*rr2* strain, KI*rr11* strain, etc.

Bioinformatics methods. The identification of histidine kinases (HKs) and response regulators (RRs) of putative TCS in the genome of GBS strain 2603 V/R was carried out using the P2CS (http://www.p2cs.org) database (42). A TCS was defined as an orphan if the predicted HK or RR gene had no adjacent partner in the locus or if the cognate partner contained any mutations (e.g., stop codons or frameshifts) that compromised the predicted gene product.

Gene sequences encoding the TCS were downloaded from the publically available genome of 2603 V/R in GenBank, except for the RR from TCS-3 and HK from TCS-17, which were downloaded from the publically available genome of CJB111. The genes used are listed in Table 1. All gene sequences were aligned against complete or draft genome sequences using FASTA version 3.4t25. A gene was considered present if the identity was >75% on at least 90% of the query sequence. Genes interrupted at the end of contigs, alignments with over 95% identity on less than 40% of the query length, and hits divided into pieces on the same contig were classified as having "ambiguity in alignment."

For polypeptide analyses, all of the genes were translated into proteins and those having mutations leading to truncated proteins were discarded. A numeric identifier was assigned to each different putatively active poly-

peptide for each gene. For each strain, a polypeptide profile of TCS was created. The goeBurst algorithm (43) was used to generate a minimum spanning tree (MST) from the profiles using Phyloviz (44). In this tree, each vertex represents a specific profile and each edge connects the profile to its closest ones.

Functional domains in each HK protein were identified by SMART and/or PFAM (http://smart.embl-heidelberg.de). Subsequently, HKs were manually assigned a signaling mechanism according to proposed criteria (8). Extracellular-sensing HKs typically have two TM helices with an intervening extracytoplasmic domain of 50 to 300 amino acids, lacking large cytoplasmic linker regions; transmembrane-sensing HKs are characterized by the presence of 2 to 20 transmembrane regions connected by very short intra- or extracellular linkers; cytoplasmic-sensing HKs include either membrane-anchored proteins that do not fulfill the criteria described above and have input domains (e.g., PAS, GAF) localized on the intracellular side or soluble HKs with no transmembrane regions.

Expression microarray analysis. Expression microarray analysis was performed using a custom-made Agilent 60-mer oligonucleotide microarray. Oligonucleotide sequences were selected with the Agilent eArray system, using 6 probes per gene. The complete set of annotated genes (2,232) in the CJB111 genome was thus covered (ftp://ftp.jcvi.org/pub/data/Microbial_Genomes/s_agalatiae_cjb111/). RNA samples used for microarray analysis were prepared as follows. Bacteria for RNA extraction (five mutant strains and the isogenic WT strain) were grown in triplicate cultures on three separate occasions. Hence, for each strain, nine independent GBS cultures (nine biological replicates obtained on three separate days) served as the source of RNA. Bacteria were harvested twice, at an OD_{600} of 0.3 (EL phase) and an OD_{600} of 1.8 to 1.9 (ES phase, ~15 min into growth arrest). To rapidly arrest transcription, 10 ml of bacteria was cooled on ice and added to 10 ml of frozen THB medium in a 50-ml conical tube. GBS cells were then collected by centrifugation for 15 min at 4,000 rpm, 4°C, and resuspended in 800 μl of TRIzol (Invitrogen). Bacteria were disrupted mechanically by agitation with lysing matrix B in 2-ml tubes (DBA Italia) using a homogenizer (FastPrep-24; MP Biomedicals) for 60 s at 6.5 m/s for two cycles, and kept on ice for 2 min between the cycles. Samples were then centrifuged for 5 min at 8,000 × *g*, 4°C, and RNA was extracted with a Direct-zol RNA miniprep kit (Zymo Research) according to the manufacturer's instructions. RNA samples were treated with DNase (Roche) for 2 h at 37°C and further purified using the RNeasy minikit (Qiagen), including a second DNase treatment on the column for 30 min at room temperature, according to the manufacturer's instructions. Five micrograms of pooled RNA from each triplicate was labeled (Cy5-dCTP/Cy3-dCTP; Euroclone) and purified (Wizard SV gel and PCR clean-up system; Promega). Labeled RNA from the three independent days of RNA extraction was then pooled and used for microarray analysis. Labeling, chip hybridization, washing, scanning, and data extraction were performed according to the procedures described by Agilent for two-color microarray-based gene expression analysis. After data acquisition, slide normalization was performed by a lowess (locally weighted scatterplot smoothing) algorithm, as implemented by the Agilent Feature Extraction software, version 9.5.3. The average log ratio of fluorescence signals [$\log_2$(Cy5/Cy3)] of probes corresponding to the same gene was computed within each slide. Student's *t* test statistics were performed to test for differentially expressed genes.

qRT-PCR analysis. cDNA was prepared using the reverse transcription system (Promega) by using 500 ng of RNA per reaction mixture volume. Real-time quantitative PCR (qRT-PCR) was performed on 50 ng of cDNA that was amplified using LightCycler 480 DNA SYBR green I master (Roche). Reactions were monitored using a LightCycler 480 instrument and software (Roche). The transcript amounts under each condition were standardized to the transcription of an internal control gene (*gyrA*) and compared with standardized expression in the wild-type strain (cycle threshold [$\Delta\Delta C_T$] method). Validation of microarray data by qRT-PCR was performed on a selection of 9 genes differentially expressed in mutant strains, using the RNA prepared for microarray analysis (see above) and primers reported in Table S1 in the supplemental material. Moreover, we prepared new RNA samples from WT, knockout, and complemented strains (three biological replicates obtained on three different days) to generate cDNA for qRT-PCR confirmation of highly regulated genes.

For RNA extraction from bacteria grown with different carbon sources, strains were first inoculated into CDM and grown at 37°C until an OD_{600} of 0.5 was reached. Cultures were harvested by centrifuging at 4,000 × *g*, 4°C, for 10 min, and each pellet was resuspended in 10 ml of CDM without glucose and split in two. Each 5-ml sample was then supplemented with 10 mg/ml of glucose or fructose-6-phosphate. The bacteria were then incubated for 30 min at 37°C, and RNA was extracted as described for the microarray analysis.

Bacterial lysate was obtained from a 10-ml culture of the WT strain in late logarithmic phase (OD of 1). Briefly, bacteria resuspended in PBS were disrupted mechanically by agitation with lysing matrix B in 2-ml tubes (DBA Italia) using a homogenizer (FastPrep-24) for 60 s at 6.5 m/s for four cycles. The tubes were kept on ice for 2 min between the cycles. Samples were centrifuged for 5 min at 8,000 × *g*, 4°C, and the supernatant was collected and designated as lysate. For the RNA extraction, strains were grown in CDM until reaching an OD_{600} of 0.5, harvested, split in two, and resuspended in 5 ml of CDM without glucose. Each sample was supplemented with 800 μl of PBS or with 800 μl of lysate for 30 min at 37°C before RNA extraction.

Phenotype microarray analysis. Phenotype microarray (PM) technology uses the irreversible chemical reduction of a patented dye as a reporter of active metabolism (45). The CJB111, Δ*rr16*, and KI*rr16* strains were used with microplates PM1 and PM2A (Biolog), testing 192 different single carbon sources. Bacteria on THB agar plates were scraped off and suspended in 5 ml of inoculation fluid (IF-0; Biolog) to an OD of 0.3. Samples were then diluted 1:10 in IF-0 to obtain a turbidity of 85% (OD of ~0.02 to 0.03) and kept on ice. Growth medium constituents were prepared according to Biolog's procedures for *S. agalactiae* and other *Streptococcus* species. PM microplates were inoculated by adding 100 μl bacterial suspension/well and then incubated for 48 h at 37°C in an OmniLog reader (Biolog). Data points were collected every 15 min. Data were then analyzed using the OmniLog software. The unspecific background (well A1 in each plate, negative control) was subtracted from the other samples.

In vivo and in vitro infection experiments. Animal studies were approved by the Office of Lab Animal Care at San Diego State University and conducted under accepted veterinary standards. Animal experiments were performed in compliance with the Novartis Animal Health and Welfare guidelines.

We adopted a previously described murine model of hematogenous GBS meningitis (28), with the difference that preliminary dose-ranging experiments established the 50% lethal dose (LD_{50}) dose of CJB111 as 1.5 × 10^7 CFU per mouse (outbred 6-week-old male CD1 mice; Charles River Laboratories). The mice were followed for 2 weeks. Also, since histopathology was not performed, we considered the experiment a model of systemic infection.

The *in vivo* mouse model of GBS vaginal colonization has been described previously (26). Female CD1 mice (8 to 16 weeks old) were obtained from Charles River Laboratories and used for colonization assays. *In vitro* adhesion was performed as previously described (26) using the immortalized human vaginal epithelial cell line VK2/E6E7, obtained from the American Type Culture Collection (ATCC CRL-2616) (46). Five to 10 passages were used for all cell assays. Cells were maintained at 37°C in a 5% CO_2 atmosphere in keratinocyte serum-free medium (KSFM; Invitrogen).

Microarray data accession numbers. The microarray chip layout was submitted to EBI ArrayExpress and is available under accession number A-MEXP-2382. Experimental results are available under accession number E-MTAB-2423.

SUPPLEMENTAL MATERIAL

Supplemental material for this article may be found at http://mbio.asm.org/lookup/suppl/doi:10.1128/mBio.00870-14/-/DCSupplemental.

Figure S1, EPS file, 0.1 MB.
Figure S2, EPS file, 0.1 MB.
Figure S3, EPS file, 0.1 MB.
Figure S4, EPS file, 0.1 MB.
Figure S5, EPS file, 1.8 MB.
Table S1, DOC file, 0.1 MB.

ACKNOWLEDGMENTS

We thank Isabel Delany for critical reading of the manuscript. We are indebted to Fabio Rigat for his input on statistical analysis. We thank Silvia Bottini for assistance with microarray data analysis. Phenotype microarray analysis was performed in the laboratory of Giacomo Romagnoli.

This work was supported by grant R01NS051247 from the NIH/NINDS to K.S.D.

REFERENCES

1. **Franciosi RA, Knostman JD, Zimmerman RA.** 1973. Group B streptococcal neonatal and infant infections. J. Pediatr. **82:**707–718. http://dx.doi.org/10.1016/S0022-3476(73)80604-3.
2. **Howard JB, McCracken GH.** 1974. The spectrum of group B streptococcal infections in infancy. Am. J. Dis. Child. **128:**815–818.
3. **Finch LA, Martin DR.** 1984. Human and bovine group B streptococci: two distinct populations. J. Appl. Bacteriol. **57:**273–278. http://dx.doi.org/10.1111/j.1365-2672.1984.tb01391.x.
4. **Dermer P, Lee C, Eggert J, Few B.** 2004. A history of neonatal group B *Streptococcus* with its related morbidity and mortality rates in the United States. J. Pediatr. Nurs. **19:**357–363. http://dx.doi.org/10.1016/j.pedn.2004.05.012.
5. **Sendi P, Johansson L, Norrby-Teglund A.** 2008. Invasive group B Streptococcal disease in non-pregnant adults: a review with emphasis on skin and soft-tissue infections. Infection **36:**100–111. http://dx.doi.org/10.1007/s15010-007-7251-0.
6. **Fernandez M, Rench MA, Albanyan EA, Edwards MS, Baker CJ.** 2001. Failure of rifampin to eradicate group B streptococcal colonization in infants. Pediatr. Infect. Dis. J. **20:**371–376. http://dx.doi.org/10.1097/00006454-200104000-00002.
7. **Maisey HC, Doran KS, Nizet V.** 2008. Recent advances in understanding the molecular basis of group B *Streptococcus* virulence. Expert Rev. Mol. Med. **10:**e27. http://dx.doi.org/10.1017/S1462399408000811.
8. **Mascher T, Helmann JD, Unden G.** 2006. Stimulus perception in bacterial signal-transducing histidine kinases. Microbiol. Mol. Biol. Rev. **70:**910–938. http://dx.doi.org/10.1128/MMBR.00020-06.
9. **Jiang SM, Cieslewicz MJ, Kasper DL, Wessels MR.** 2005. Regulation of virulence by a two-component system in group B *Streptococcus*. J. Bacteriol. **187:**1105–1113. http://dx.doi.org/10.1128/JB.187.3.1105-1113.2005.
10. **Lamy MC, Zouine M, Fert J, Vergassola M, Couve E, Pellegrini E, Glaser P, Kunst F, Msadek T, Trieu-Cuot P, Poyart C.** 2004. CovS/CovR of group B *Streptococcus*: a two-component global regulatory system involved in virulence. Mol. Microbiol. **54:**1250–1268. http://dx.doi.org/10.1111/j.1365-2958.2004.04365.x.
11. **Jiang SM, Ishmael N, Dunning Hotopp J, Puliti M, Tissi L, Kumar N, Cieslewicz MJ, Tettelin H, Wessels MR.** 2008. Variation in the group B *Streptococcus* CsrRS regulon and effects on pathogenicity. J. Bacteriol. **190:**1956–1965. http://dx.doi.org/10.1128/JB.01677-07.
12. **Di Palo B, Rippa V, Santi I, Brettoni C, Muzzi A, Metruccio MM, Grifantini R, Telford JL, Paccani SR, Soriani M.** 2012. Adaptive response of group B *Streptococcus* to high glucose conditions: new insights on the CovRS regulation Network. PLoS One **8:**e61294. http://dx.doi.org/10.1371/journal.pone.0061294.
13. **Quach D, van Sorge NM, Kristian SA, Bryan JD, Shelver DW, Doran KS.** 2009. The CiaR response regulator in group B *Streptococcus* promotes intracellular survival and resistance to innate immune defenses. J. Bacteriol. **191:**2023–2032. http://dx.doi.org/10.1128/JB.01216-08.
14. **Rozhdestvenskaya AS, Totolian AA, Dmitriev AV.** 2010. Inactivation of DNA-binding response regulator Sak189 abrogates beta-antigen expression and affects virulence of *Streptococcus agalactiae*. PLoS One **5:**e10212. http://dx.doi.org/10.1371/journal.pone.0010212.
15. **Klinzing DC, Ishmael N, Dunning Hotopp JC, Tettelin H, Shields KR, Madoff LC, Puopolo KM.** 2013. The two-component response regulator LiaR regulates cell wall stress responses, pili expression and virulence in group B *Streptococcus*. Microbiology **159:**1521–1534. http://dx.doi.org/10.1099/mic.0.064444-0.
16. **Poyart C, Lamy MC, Boumaila C, Fiedler F, Trieu-Cuot P.** 2001. Regulation of D-alanyl-lipoteichoic acid biosynthesis in *Streptococcus agalactiae* involves a novel two-component regulatory system. J. Bacteriol. **183:**6324–6334. http://dx.doi.org/10.1128/JB.183.21.6324-6334.2001.
17. **Spellerberg B, Rozdzinski E, Martin S, Weber-Heynemann J, Lütticken R.** 2002. *rgf* encodes a novel two-component signal transduction system of *Streptococcus agalactiae*. Infect. Immun. **70:**2434–2440. http://dx.doi.org/10.1128/IAI.70.5.2434-2440.2002.
18. **Safadi Al R, Mereghetti L, Salloum M, Lartigue M-F, Virlogeux-Payant I, Quentin R, Rosenau A.** 2010. Two-component system RgfA/C activates the *fbsB* gene encoding major fibrinogen-binding protein in highly virulent CC17 clone group B *Streptococcus*. PLoS One **6:**e14658. http://dx.doi.org/10.1371/journal.pone.0014658.
19. **Zaleznik DF, Rench MA, Hillier S, Krohn MA, Platt R, Lee ML, Flores AE, Ferrieri P, Baker CJ.** 2000. Invasive disease due to group B *Streptococcus* in pregnant women and neonates from diverse population groups. Clin. Infect. Dis. **30:**276–281. http://dx.doi.org/10.1086/313665.
20. **Galperin MY.** 2010. Diversity of structure and function of response regulator output domains. Curr. Opin. Microbiol. **13:**150–159. http://dx.doi.org/10.1016/j.mib.2010.01.005.
21. **Ahn SJ, Qu MD, Roberts E, Burne RA, Rice KC.** 2012. Identification of the *Streptococcus mutans* LytST two-component regulon reveals its contribution to oxidative stress tolerance. BMC Microbiol. **12:**187. http://dx.doi.org/10.1186/1471-2180-12-187.
22. **Ahn SJ, Rice KC, Oleas J, Bayles KW, Burne RA.** 2010. The *Streptococcus mutans* Cid and Lrg systems modulate virulence traits in response to multiple environmental signals. Microbiology **156:**3136–3147. http://dx.doi.org/10.1099/mic.0.039586-0.
23. **van de Rijn I, Kessler RE.** 1980. Growth characteristics of group A streptococci in a new chemically defined medium. Infect. Immun. **27:**444–448.
24. **Watson ME, Nielsen HV, Hultgren SJ, Caparon MG.** 2013. Murine vaginal colonization model for investigating asymptomatic mucosal carriage of *Streptococcus pyogenes*. Infect. Immun. **81:**1606–1617. http://dx.doi.org/10.1128/IAI.00021-13.
25. **Patras KA, Wang NY, Fletcher EM, Cavaco CK, Jimenez A, Garg M, Fierer J, Sheen TR, Rajagopal L, Doran KS.** 2013. Group B *Streptococcus* CovR regulation modulates host immune signalling pathways to promote vaginal colonization. Cell. Microbiol. **15:**1154–1167. http://dx.doi.org/10.1111/cmi.12105.
26. **Sheen TR, Jimenez A, Wang NY, Banerjee A, van Sorge NM, Doran KS.** 2011. Serine-rich repeat proteins and pili promote *Streptococcus agalactiae* colonization of the vaginal tract. J. Bacteriol. **193:**6834–6842. http://dx.doi.org/10.1128/JB.00094-11.
27. **Doran KS, Engelson EJ, Khosravi A, Maisey HC, Fedtke I, Equils O, Michelsen KS, Arditi M, Peschel A, Nizet V.** 2005. Blood-brain barrier invasion by group B *Streptococcus* depends upon proper cell-surface anchoring of lipoteichoic acid. J. Clin. Invest. **115:**2499–2507. http://dx.doi.org/10.1172/JCI23829.
28. **Doran KS, Liu GY, Nizet V.** 2003. Group B streptococcal beta-hemolysin/cytolysin activates neutrophil signaling pathways in brain endothelium and contributes to development of meningitis. J. Clin. Invest. **112:**736–744. http://dx.doi.org/10.1172/JCI200317335.
29. **Schubert A, Zakikhany K, Schreiner M, Frank R, Spellerberg B, Eikmanns BJ, Reinscheid DJ.** 2002. A fibrinogen receptor from group B *Streptococcus* interacts with fibrinogen by repetitive units with novel ligand binding sites. Mol. Microbiol. **46:**557–569. http://dx.doi.org/10.1046/j.1365-2958.2002.03177.x.
30. **Schubert A, Zakikhany K, Pietrocola G, Meinke A, Speziale P, Eikmanns BJ, Reinscheid DJ.** 2004. The fibrinogen receptor FbsA promotes adherence of *Streptococcus agalactiae* to human epithelial cells. Infect. Immun. **72:**6197–6205. http://dx.doi.org/10.1128/IAI.72.11.6197-6205.2004.
31. **Springman AC, Lacher DW, Wu G, Milton N, Whittam TS, Davies HD, Manning SD.** 2009. Selection, recombination, and virulence gene diversity among group B streptococcal genotypes. J. Bacteriol. **191:**5419–5427. http://dx.doi.org/10.1128/JB.00369-09.
32. **Webber CA, Kadner RJ.** 1997. Involvement of the amino-terminal phos-

phorylation module of UhpA in activation of *uhpT* transcription in *Escherichia coli*. Mol. Microbiol. **24:**1039–1048. http://dx.doi.org/10.1046/j.1365-2958.1997.4021765.x.

33. **Zhou L, Lei XH, Bochner BR, Wanner BL.** 2003. Phenotype microarray analysis of *Escherichia coli* K-12 mutants with deletions of all two-component systems. J. Bacteriol. **185:**4956–4972. http://dx.doi.org/10.1128/JB.185.16.4956-4972.2003.
34. **Barelle CJ, Priest CL, Maccallum DM, Gow NA, Odds FC, Brown AJ.** 2006. Niche-specific regulation of central metabolic pathways in a fungal pathogen. Cell. Microbiol. **8:**961–971. http://dx.doi.org/10.1111/j.1462-5822.2005.00676.x.
35. **Muñoz-Elías EJ, McKinney JD.** 2005. *Mycobacterium tuberculosis* isocitrate lyases 1 and 2 are jointly required for *in vivo* growth and virulence. Nat. Med. **11:**638–644. http://dx.doi.org/10.1038/nm1252.
36. **Lau GW, Haataja S, Lonetto M, Kensit SE, Marra A, Bryant AP, McDevitt D, Morrison DA, Holden DW.** 2001. A functional genomic analysis of type 3 *Streptococcus pneumoniae* virulence. Mol. Microbiol. **40:**555–571. http://dx.doi.org/10.1046/j.1365-2958.2001.02335.x.
37. **Polissi A, Pontiggia A, Feger G, Altieri M, Mottl H, Ferrari L, Simon D.** 1998. Large-scale identification of virulence genes from *Streptococcus pneumoniae*. Infect. Immun. **66:**5620–5629.
38. **Tchawa Yimga M, Leatham MP, Allen JH, Laux DC, Conway T, Cohen PS.** 2006. Role of gluconeogenesis and the tricarboxylic acid cycle in the virulence of *Salmonella enterica* serovar Typhimurium in BALB/c mice. Infect. Immun. **74:**1130–1140. http://dx.doi.org/10.1128/IAI.74.2.1130-1140.2006.
39. **Perez-Casal J, Price JA, Maguin E, Scott JR.** 1993. An M protein with a single C repeat prevents phagocytosis of *Streptococcus pyogenes*: use of a temperature-sensitive shuttle vector to deliver homologous sequences to the chromosome of *S. pyogenes*. Mol. Microbiol. **8:**809–819. http://dx.doi.org/10.1111/j.1365-2958.1993.tb01628.x.
40. **Horton RM, Hunt HD, Ho SN, Pullen JK, Pease LR.** 1989. Engineering hybrid genes without the use of restriction enzymes: gene splicing by overlap extension. Gene **77:**61–68. http://dx.doi.org/10.1016/0378-1119(89)90359-4.
41. **Framson PE, Nittayajarn A, Merry J, Youngman P, Rubens CE.** 1997. New genetic techniques for group B streptococci: high-efficiency transformation, maintenance of temperature-sensitive pWV01 plasmids, and mutagenesis with Tn917. Appl. Environ. Microbiol. **63:**3539–3547.
42. **Barakat M, Ortet P, Jourlin-Castelli C, Ansaldi M, Méjean V, Whitworth DE.** 2009. P2CS: a two-component system resource for prokaryotic signal transduction research. BMC Genomics **10:**315. http://dx.doi.org/10.1186/1471-2164-10-315.
43. **Francisco AP, Bugalho M, Ramirez M, Carriço JA.** 2009. Global optimal eBURST analysis of multilocus typing data using a graphic matroid approach. BMC Bioinformatics **10:**152. http://dx.doi.org/10.1186/1471-2105-10-152.
44. **Francisco AP, Vaz C, Monteiro PT, Melo-Cristino J, Ramirez M, Carriço JA.** 2012. PHYLOViZ: phylogenetic inference and data visualization for sequence based typing methods. BMC Bioinformatics **13:**87. http://dx.doi.org/10.1186/1471-2105-13-87.
45. **Bochner BR, Gadzinski P, Panomitros E.** 2001. Phenotype microarrays for high-throughput phenotypic testing and assay of gene function. Genome Res. **11:**1246–1255. http://dx.doi.org/10.1101/gr.186501.
46. **Fichorova RN, Rheinwald JG, Anderson DJ.** 1997. Generation of papillomavirus-immortalized cell lines from normal human ectocervical, endocervical, and vaginal epithelium that maintain expression of tissue-specific differentiation proteins. Biol. Reprod. **57:**847–855. http://dx.doi.org/10.1095/biolreprod57.4.847.